An Improved Methodological Approach for Denoising of Partial Discharge Data by the Wavelet Transform

Carlo Petrarca* and Giovanni Lupò

Abstract—Partial Discharge (PD) measurements may be affected by external noise and disturbances of various natures such as interference from broadcasting stations, stochastic noise, pulses from power electronics, etc. Extracting PD pulses from such a noisy environment is therefore a crucial issue. This paper presents a wavelet based technique for automatic noise rejection. The core of the paper is the use of an improved methodological approach for the selection of a suitable wavelet, which aims at summing up the benefits and overcoming some limitations of previous techniques. Firstly, a very wide set of training signals is used for the identification of the decomposition level and for the calculation of suitable performance parameters that identify each wavelet; then a Performance Fingerprint is introduced in order to summarize the ability of a specific wavelet to reconstruct a partial discharge waveform, and a distance criterion is used for the selection of the most suitable wavelet. Afterwards, useful information is collected for the reconstruction of the PD signal, and finally, results on the application of the algorithm for a set of numerical and experimental signals are presented.

1. INTRODUCTION

Partial discharge detection is a powerful non-destructive diagnostic tool, able to provide vital information on the status of electrical equipment. In particular, it is able to identify the nature of those defects in the insulation system which can lead to a premature failure of the electrical components [1].

PD detection involves the acquisition, storage and processing of a series of transient, irregular, non-periodic electrical pulses, whose characteristics depend on the entity of the discharge phenomena, on its site of origin and its detection point, on the frequency response of the detector, on the bandwidth of the amplifier, etc. [2].

Generally, the measurements are carried out in shielded laboratories, with filtered power supplies and under applied voltages which are generally higher than the normal operational voltage. In such a controlled electromagnetic environment, for an expert operator, it is not difficult to ascertain the presence of PD activity. When PD measurements are performed outside laboratories, noise and interference can be severe under operating conditions: disturbances can derive from corona phenomena, from communication systems, from power electronics, etc. In such cases PDs can be completely buried in low Signal to Noise Ratio (SNR) signals.

In order to suppress such undesirable signals, some hardware solutions have been proposed, such as detectors with limited bandwidth ($< 500\,\text{kHz}$), but most noises still cannot be rejected; furthermore, the use of narrower bandwidths is not recommended since the PD pulse resolution is strongly reduced and misleading results can be obtained, especially when the repetition rate of the PD signals is high. Balanced bridge arrangements have also been suggested in order to reject external noise, but they require critical adjustments (i.e., the bridge balancing) or additional equipment.

The rapid development of high-speed computers has made software-based rejection tools much more attractive. They are post-processing tools which are mainly based on the knowledge about the difference between the nature of PD signals and the nature of external noise. In particular, if rough information is known about the characteristics of the signal to be extracted (i.e., bandwidth, waveform, etc.), good results can be obtained. Traditionally, the unwanted signals have been suppressed using filtering techniques based on the Fourier Transform (FT) or Short-Time Fourier Transform (STFT) [3, 4]; however, the non-periodical and transient nature of PD signals makes it more promising the use of a filtering technique based on the Wavelet Transform (WT), which involves multiresolution decomposition of measured data into wavelet coefficients, each having unique time and frequency information [5].

The authors already published results [6] on the application of a discrete version of the Wavelet Transform, the so-called Discrete Wavelet Transform (DWT), for the analysis of UltraWide-Band (UWB) PD current signals. They also published papers presenting the use of Wavelet Packet Transform (WPT) [7], generalization of the DWT, for noise suppression and subsequent PD extraction [8–10]: their analysis, however, was limited only to numerical signals. WPT has also been used recently for UWB impulse radio signal denoising [11], although the authors do not comment on possible limitations and drawback of the adopted technique. Satish and Nazneen [12] used the DWT for extracting PD pulses buried in very high levels of noise and interferences and showed that the results obtained with the proposed wavelet-based denoising technique were superior with respect to those obtained with different digital filtering approaches, such as the FIR (Finite Impulse Response) method and the IIR (Infinite Impulse Response)-notch filter method. In the paper they underlined the importance for best results of an optimal choice of the mother wavelet and of the number of levels for decomposition-reconstruction of the input signal, but they did not deal with such a topic.

In [13] three types of wavelet transform methods (i.e., Discrete Wavelet Transform, Wavelet Packet Transform and Stationary Wavelet Transform) were compared when applied to simulated PD data, but only the presence of white noise and of sinusoidal interference was taken into account. The authors concluded their paper by asserting that the best trade-off between the denoising effect and the computing time was DWT, thus explaining the great interest it had attracted. In [14] Ma et al. proposed a methodology for comparing the performances of each wavelet. They used only two types of training signals for testing the performance of each wavelet and the choice of the most suitable one was based on an energy criterion and on the calculation of only one parameter, namely the correlation coefficient between the original and the reconstructed pulse.

An improved methodology applied to narrow band PD detection was proposed by Zhou et al. [15]; it was founded on the knowledge of the frequency spectrum of the expected PD pulse, on the calculation of the PD energy distribution after digital filtering and on hard thresholding for the choice of suitable wavelet coefficients. In the paper the effectiveness of the filtering technique was evaluated only on one type of simulated PD pulse corrupted by different levels of noise. Most of the reproduced noise signal was unfortunately characterized by a significant frequency content outside the bandwidth of a typical narrow band receiver, which means that the denoising performance of the method were not completely clarified.

Good results were reported by Kyprianou et al. [16] by introducing the Wavelet Packet Transform (WPT), but for a proper choice of the mother wavelet the authors considered PDs corrupted only by different levels of white noise, thus not including the great variety of noise and disturbances affecting partial discharge measurements. More recently Macedo et al. [18] used the cross correlation factor as a unique performance parameter for the choice of an appropriate mother-wavelet, while in [17] Chang et al. put in evidence that the possible reason for bad performances of the denoising techniques could be ascribed to a limited set of training signals or to an inadequate selection of the performing parameters.

The aim of the present paper is to overcome some of the limitations of the methods illustrated above by exploiting the main features of Discrete Wavelet Transform de-noising. In particular the performance of each wavelet will be investigated with a set of a significant number of training signals, representing typical PD pulses acquired with a conventional narrow band detector, having different amplitudes, polarities, frequency contents, time-shift or time intervals between two successive pulses, etc. Moreover, a much wider set of performance parameters will be considered for choosing the optimal wavelet and afterwards a Performance Fingerprint will be defined as a compressed information on the ability of a specific wavelet to reconstruct a partial discharge waveform. Finally a distance criterion will

be adopted for the choice of the most suitable wavelet for PD denoising.

The paper is organized as follows: after the present introduction, in Section 2 a brief description of the Wavelet Transform is given; in the third section the improved methodology for wavelet selection is presented; the fourth part is dedicated to the presentation of numerical and experimental results, while in the last section the conclusions are given and further research directions are discussed.

2. A BRIEF INTRODUCTION TO WAVELET TRANSFORM

Wavelets (ondelettes in French, small waves in English) are a set of functions used to represent transient phenomena that result from a dilation and shift of the original waveform [19]. The Wavelet Transform (WT) is a mathematical tool, particularly designed to analyze transient, irregular and non-periodical signals (i.e., partial discharge pulses). While the Fourier Transform (FT) decomposes the signal into sine waves of various frequency, the Wavelet Transform breaks up the signal into shifted and scaled versions of a mother wavelet. The Continuous Wavelet Transform (CWT) of a signal $s(t)$ is linear time-frequency transform expressed as:

$$\text{CWT}(a, b) = \frac{1}{\sqrt{|a|}} \int_{-\infty}^{+\infty} h\left(\frac{t - b}{a}\right) \cdot s(t) \cdot dt \tag{1}$$

where $h(t)$ is the mother wavelet, a the scale parameter, and b the shift operator. The scale parameter is related to the reciprocal of frequency and the translation parameter stands for time. Many coefficients are the result of such an operation; they are function of scale and position and depend on the waveshape of the mother wavelet. The value of each wavelet coefficient represents the similarity between the examined section of $s(t)$ and the scaled and shifted mother wavelet. Thus, differently from the Fourier Transform, which can give only frequency information, the Wavelet Transform can provide information in time and frequency simultaneously.

However, calculating wavelet coefficients at every scale is a great amount of work and generates a lot of data with consequent computational effort and redundancy. In order to overcome such drawbacks, the Discrete Wavelet Transform (DWT) is introduced by choosing only a subset of scale and time shifts. In particular, scales a and shifts b are evaluated as follows:

$$\begin{cases} a = 2^m \\ b = n2^m \end{cases} \tag{2}$$

with m, n integer values, which means that scales and positions are based on powers of two, thus avoiding time consuming and eliminating redundancies and obtaining an efficient analysis with equal accuracy [20].

Performing a DWT is equivalent to filtering the signal $s(t)$ by two filters, a high pass filter HF (to analyze the high frequency component Ds, called detail) and a low pass filter LF (to analyze the low frequency component As, called approximation).

The two filters are quadrature mirror filters (QMF), which are half-band filters, whose spectrum is symmetrical around the mid-point angular frequency $\pi/2$. Now, since the bandwidth of $s(t)$ has been reduced by a factor of two after filtering, the outcoming signal Ds and As can be sampled by a factor of two without any aliasing, according to the Nyquist theorem.

The approximations and details may be extracted using a successive filtering scheme. In particular, the original signal is passed through the two QMF to get two signals. The high-pass filter yields the first level detail signal and the low-pass filter yields the first level approximation signal. In order to eliminate redundancy, the two signals are downsampled by a factor of two. The filtering and downsampling can be repeated on the first level approximation coefficients (the downsampled low-pass output) to yield the second level approximation and detail coefficients ($As2$, $Ds2$). If one continues to filter and downsample each successive approximation, the scale is increased by a factor of two at each level of analysis. A DWT at level 1 yields the detail at the scale 21, a DWT at level 2 yields the detail at the scale 22, and so on (Figure 1).

In the present paper, the Discrete Wavelet Transform is proposed as a tool for the processing of signals acquired during on-site PD measurements. The idea underlying the de-noising technique is that,
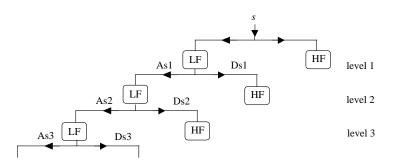
Figure 1. WT decomposition tree.

after the wavelet decomposition, the characteristics of the PD pulses and those of noise signals and interferences can be easily distinguished, thus allowing the extraction of the signal of interest. In fact, for a PD pulse coming from a conventional band detector, there is a specific frequency band in which the PD waveform is located and such a characteristic could correspond to a specific node and to a specific level in the decomposition tree, thus allowing the identification of the desired signal. In the following section the criterion for the selection of the most suitable wavelet will be described.

3. WAVELET SELECTION

The choice of the mother wavelet is a crucial point. We started from a set of candidate wavelet families already used by other authors [12, 13, 15, 17] such as Daubechies (db), Symlets (sym), Biorthogonal (bio), Coiflets (coif); in particular, by taking into account wavelets of different orders, the performances of a total number of 60 wavelets were compared.

   In the present paper we propose a procedure summarized in five steps for the identification of the Most Suitable Wavelet (MSW):

1) identification of the set T of training PD pulses;
2) selection of decomposition level L_d;
3) computation of performance parameters $[p_1, p_2, p_3, \ldots, p_i, \ldots]$ of each wavelet;
4) implementation of distance criterion for selection of MSW;
5) thresholding of wavelet coefficients.

3.1. Set of Training PD Pulses

Partial Discharges are breakdown phenomena that do not completely bridge the distance between two electrodes. Different types of PDs can be distinguished, such as internal discharges, surface discharges, corona discharges etc. [21]. Every discharge type has its own development and behavior, depending on the physical phenomenon that is taking place and on the surrounding boundary conditions. As a consequence, the discharge impulses may have very different shapes and time behaviors [22].

   Classical electrical detection of partial discharges makes use of RCL or RC pulse detectors of limited bandwidth of about 100 to 500 kHz. In this case, discharges are displayed as short impulses whose shape is independent of the physical process of the discharge and is determined only by the detection circuit parameters [21]. As a consequence, we can define a "typical recorded PD signal" $s(t)$ which appears as a damped oscillatory narrow band pulse.

   In the case of an RC detector with a limited bandwidth [40–400] kHz, as suggested by other authors [12], it can be expressed as:

$$s\left(t\right) = \begin{cases} 0 & t < t_0 \\ A \cdot e^{-\frac{t-t_0}{\tau}} \sin\left[2\pi f_0\left(t - t_0\right)\right] & t \geq t_0 \end{cases} \tag{3}$$

where A is the amplitude of the pulse, f_0 its frequency, τ the damping factor, and t_0 the time instant of pulse occurrence. Different PD pulse shapes were chosen as test-waveform in order to take into account

the response of a great number of commercially available PD detectors: the damping factor τ was chosen among 2, 5, and 10 μs and the frequency f_0 chosen among 150, 200 and 250 kHz, so creating a primary test-set T_1 of $N_{t1} = 9$ different waveforms. Moreover, different sequences of such pulses were considered (i.e., two or three pulses, pulses of different amplitudes, etc.) thus adding a secondary test-set T_2 of $N_{t2} = 36$ cases to be used for the choice of the most suitable mother wavelet. The overall test-set $T = T_1 \cup T_2$ was thus composed of $N_t = N_{t1} + N_{t2} = 45$ waveforms.

A typical conventional waveform $s(t)$, belonging to the primary test-set T_1, is reported in Figure 2(a) ($f_0 = 200$ kHz, $\tau = 5$ μs, $t_0 = 30$ μs), while in Figure 2(b) an example of a signal belonging to test-set T_2 is shown ($f_0 = 150$ kHz, $\tau = 10$ μs, $t_0 = 30$ μs). For a better readability of the figures, the time-scales are different in Figure 2(a) and Figure 2(b), but we remark that in all examples the time-scale was set at 1 ms and the sampling frequency f_s was chosen equal to $f_s = 20$ MHz.
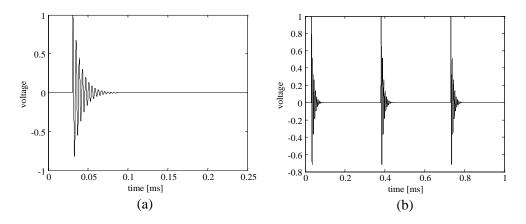

Figure 2. (a) PD waveform in test-set T_1; (b) PD waveform in test-set T_2.

3.2. Selection of the Decomposition Level

As a first step, for all the 60 candidate wavelets, each single PD pulse of test-set $T = T_1 \cup T_2$ was decomposed down to its maximum level, and the energy distribution of the signal was calculated in each subsequence. Energy is allocated at different percentages in each approximation and detail node of a specific level; the ideal condition is obtained when at the deepest decomposition level the energy is contained in a unique node n^*: in such a case n^* can be considered as peculiar of the PD pulse and only such a node can be used for signal reconstruction by performing the Inverse Transform algorithm. Such an ideal condition is never fulfilled, as in Figure 3, where the energy distribution in the approximation node of 6th level as a function of the mother wavelets is shown; it is possible to notice that the *percentage*
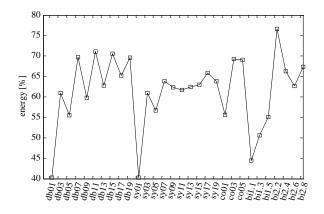

Figure 3. Energy content at approximation node of 6th level vs. mother wavelets.

energy content (*pec*) is in many cases sensibly lower than 80%, which means that great part of energy is lost as a consequence of filtering. Please, note that in Figure 3, for the sake of clarity, on the x-axis only 30 wavelets have been selected.

Since level $n.$ 5 is the lowest level in which, despite the previous successive filtering, almost all energy of the signal is concentrated in a unique approximation node n^*, it was chosen as reference level L_d for the decomposition, while the percentage energy content *pec* of the corresponding node was set as the first performance parameter p_{1j} associated to the j-th wavelet.

3.3. Computation of Performance Parameters

In order to assess the feature of the j-th wavelet, besides p_{1j}, two further parameters were added:

a) the percentage cross correlation factor (*pcc*) between the original (S) and the signal (R) reconstructed by using node n^*, which indicates the degree of similarity between S and R,

$$pcc = \frac{\sum_{i=0}^{N-1} \left(R(i) - \bar{R} \right) \left(S(i) - \bar{S} \right)}{\sqrt{\sum_{i=0}^{N-1} \left(R(i) - \bar{R} \right)^2 \left(S(i) - \bar{S} \right)^2}} * 100 \tag{4}$$

where N is the length of the signal, $\bar{R}$ the mean value of R, and $\bar{S}$ the mean value of S. A value of *pcc* $= 100$ means 100% shape similarity, while $pcc = 0$ means total asymmetry between the signals.

b) the percentage complementary error (*pce*) on the peak amplitude,

$$pce = 100 - \Delta E\% = 100 - \left| \frac{S_M - R_M}{S_M} \right| * 100 \tag{5}$$

where $\Delta E\%$ is the percentage error on the maximum values, R_M the maximum value of R, and S_M the maximum value of S. A value of $pce = 100$ means that the maximum value of the original signal has been reproduced with no error. If a waveform contains k PD test-signals, the *pce* is calculated on each of k peak amplitudes. We remark that the evaluation of *pce* is extremely important since in narrow band detection systems the peak of the PD signal is an indirect measure of apparent charge [1].

Once fixed the j-th wavelet, the three performance parameters (*pec*, *pcc*, *pce*) defined above were calculated for each of the 45 training waveforms in T, resulting in a set of $M = 45 \times 3 = 135$ variables that describe the ability of the single wavelet to reproduce a partial discharge signal. Such a set of parameters can be named as *Performance Fingerprint* (*PF*), so recalling a term which is well known in PD recognition and classification [23, 24]. In the next paragraph *PF* will be used as a discrimination tool among the wavelets.

3.4. Distance Criterion

The *Performance Fingerprint* represents compressed information on the ability of a specific wavelet to reconstruct a partial discharge waveform. We can define the *Optimal Performance Fingerprint* (*OPF*) as a set of performance parameters *op* all equal to 100, which corresponds to a perfect reconstruction for the original signal:

$$OPF: op_i = 100 \quad i = 1 : 135 \tag{6}$$

OPF can be represented in a 135-dimensional parameter space.

The generic j-th *PF*, calculated by adopting the j-th wavelet, occupies a well-defined position in such a multidimensional space; we can easily compare it to the information produced by other wavelets. In fact, if we define the Euclidean distance d_{io} between each *PF* and the optimal fingerprint *OPF* as:

$$d_{io} = \sqrt{\sum_{i=1}^{M=135} (p_i - op_i)^2} \tag{7}$$
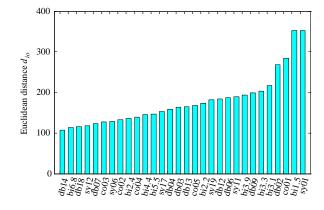
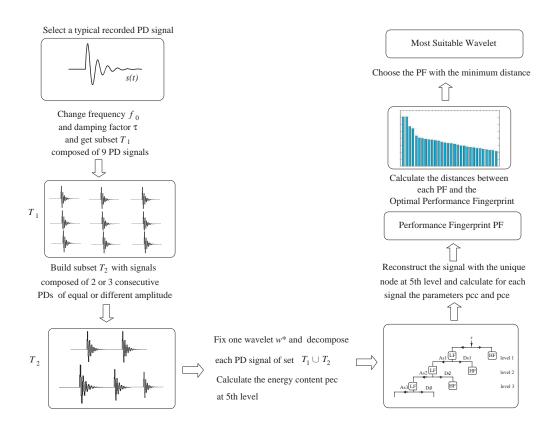**Figure 4.** Euclidean distances d_{i0} for different wavelets.

Figure 5. The main steps of the adopted procedure.

the idea underlying the identification of the *Most Suitable Wavelet* (*MSV*) is to evaluate and select the wavelet whose *Performance Fingerprint* has the minimum distance from *OPF*. The results of the calculation of the Euclidean distances are summarized in Figure 4 where, for better readability of the image, only some of the wavelets are reported.

We can notice that the Performance Fingerprints of wavelets, such as *sys01* and *bior1.5*, are extremely far ($d_{i0} > 360$) from the optimal *OPF*, while the *Performance Fingerprint* with the minimum distance ($d_{i0} = 108$) from *OPF* is obtained with the Daubechies wavelet *db14*, with a 5th level decomposition. It means that the reconstruction of the original signal $s(t)$ by *db14* is the closest to the perfect reconstruction. For such a reason, wavelet *db14* was elected as *Most Suitable Wavelet* (*MSV*).

For the sake of clarity, in Figure 5 the main steps of the adopted procedure are summarized.

3.5. Thresholding of Wavelet Coefficients

Among all the wavelet coefficients describing the PD waveform at approximation node n^*, only a few of them carries significant information on the PD. Hard-thresholding can thus be employed, that is, if a coefficient value is lower than a preset limit (defined by the thresholding rules), it is set to zero and discarded in the Inverse Transform.

In order to select the threshold, all the coefficients calculated at node n^* at level 5 were ordered in a descending rule, from the highest to the lowest. Then, an Inverse Transform was performed by using the first, and highest coefficient, and the signal Y_1 was extracted; finally the parameters *pcc* and *pce* were calculated, by comparing Y_1 with the original signal S. The same steps were repeated by adding a new coefficient each time: for example, at k-th step, k wavelet coefficients are used for the extraction of signal Y_k and the parameters are then calculated. It is possible to observe that by adding coefficients whose value is lower than 0.05, improvements lower than 1% can be obtained in the performance parameters, thus suggesting that a threshold $\sigma = 0.05$ can be set, without losing information on the waveform of the PD signal.

An example of reconstruction by *db14* and hard-thresholding is shown in Figure 6(a) and Figure 6(b), in which the input PD test signals that were reconstructed are those depicted in Figure 2.
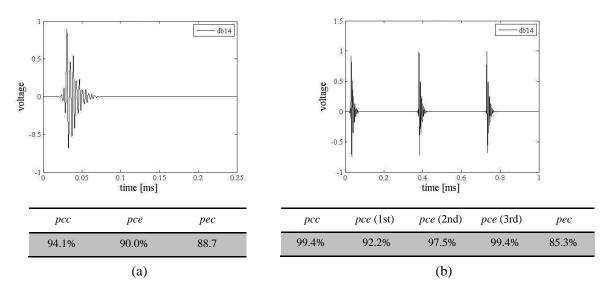

pcc	*pce*	*pec*
94.1%	90.0%	88.7

(a)

pcc	*pce* (1st)	*pce* (2nd)	*pce* (3rd)	*pec*
99.4%	92.2%	97.5%	99.4%	85.3%

(b)

Figure 6. (a) Reconstruction of PD waveform in set T_1; (b) in set T_2 and corresponding performance parameters.

Each figure is accompanied by a table reporting the calculated performance parameters. We can notice that even in the case of a complex signal (Figure 6(b)), we can get a highly satisfactory reconstruction.

The whole procedure of wavelet selection is completed in about 3 minutes by using a computer equipped with a Core 2 Duo 2.8 GHz processor and 2 GB of RAM. It must be performed only once, depending on the measurement setup. In particular, it can be easily adopted when using a narrow band PD detection system which complies with IEC 60270 standard, since in this case the output signals have predictable wave shape. We explicitly remark that the whole procedure must be repeated, by following the same steps, if a PD detector with a different bandwidth has to be used, since a new suitable set T of training pulse has to be considered.

4. PD PULSE EXTRACTION FROM NOISE

In order to prove the efficiency of the described method for wavelet selection, both numerical and experimental tests were carried out, with one or more discharge pulses submerged by noise and external

interferences.

In the numerical simulations the following steps were implemented: 1) the measured signal was decomposed down to the 5th level by the wavelet *db14*; 2) the approximation node was selected; 3) only the coefficients whose value is higher than the threshold $\sigma = 0.05$ were chosen; 4) Inverse Transform was performed; 5) performance parameters were calculated.

4.1. Numerical Results

In the numerical simulations the external disturbances were all composed of white noise of zero mean, and of typical interferences generated as amplitude modulated sine-waves of various frequency (162 kHz, 252 kHz, 548 kHz, 648 kHz, 765 kHz) with 40% modulation, and constant modulating frequency of 1 kHz [12]. All simulations refer to a typical time window of 1 ms and a sampling frequency of 20 MHz. In order to measure the extent of noiseness, the Signal to Noise Ratio SNR (dB) was used:

$$\text{SNR (dB)} = 10 * \log_{10} \frac{W_S}{W_n} \tag{8}$$

where W_S and W_n are the energy of PD signal and noise, respectively.

The following examples are a selection of test cases that try to put in evidence the efficiency of the proposed method. For each case the calculated performance parameters are reported.

1) One PD

One normalized PD signal ($\tau = 10\,\mu s$, $f_0 = 150\,\text{kHz}$) (Figure 7(a)) submerged in external noise (SNR $-15\,\text{dB}$) (Figure 7(b)). The reconstructed PD signal (Figure 7(c)) is characterized by $pcc = 78.5\%$ and $pce = 94.5\%$.
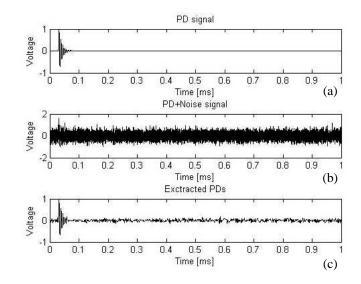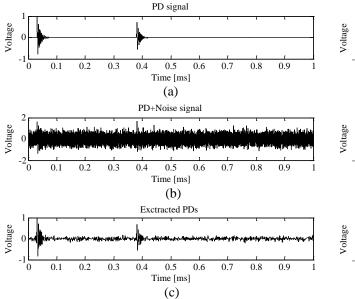

Figure 7. (a) PD signal; (b) PD submerged by noise (SNR $= -15\,\text{dB}$); (c) extracted PD.

It is possible to evaluate the efficiency of the denoising procedure by comparing the performance of wavelet *bior3.1* which, according to the sole energy criterion, can be selected as the most suitable wavelet. In fact, at 5th level it has the highest percentage energy content $pec = 97\%$. In this case, the extraction of the PD signal from noise is characterized by $pcc = 15.3\%$ and $pce = 59.4\%$ which certainly correspond to an unsatisfactory reconstruction of the original signal.

2) Two PDs of different amplitudes

Two PDs ($\tau = 10\,\mu s$, $f_0 = 200\,\text{kHz}$) of different amplitudes (1 and 0.7, respectively), shifted in time ($\Delta t = 350\,\mu s$), (Figure 8(a)) are submerged in external noise (SNR $-15\,\text{dB}$) (Figure 8(b)). The reconstruction of the PD signals (Figure 8(c)) is characterized by $pcc = 78.1\%$ pce (1st pulse) $= 96.4\%$, pce (2nd pulse) $= 95.2\%$.
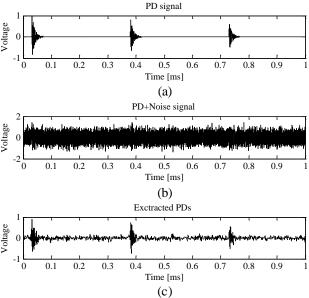
Figure 8. (a) Two PD signals; (b) PDs submerged by noise (SNR = −15 dB); (c) extracted PDs.

Figure 9. (a) Three PD signals; (b) PDs submerged by noise (SNR = −20 dB); (c) extracted PDs.

3) Three PDs of different amplitudes

Three PDs ($\tau = 10\,\mu$s, $f_0 = 250$ kHz) of different amplitudes (1.0, 0.8, 0.6) and shifted in time (Figure 9(a)) are hidden in external noise and interferences (SNR = −20 dB) (Figure 9(b)). The restored pulses are characterized by $pcc = 75\%$; pce (1st pulse) = 98%, pce (2nd pulse) = 89.6%, pce (3rd pulse) = 66.7%, (Figure 9(c)).

By a careful analysis of all 45 test waveforms submerged by noise, it was found that the quality of reconstruction was satisfactory concerning evaluation of the two first peaks, with an average value of the performance parameters equal to pce (1st pulse) = 89.0% and pce (2nd pulse) = 87.2%. The worst result was obtained with the evaluation of the peak of the third pulse, characterized by an average value pce (3rd pulse) = 80.0%.

4.2. Experimental Results

Experimental tests were carried out in the High Voltage Laboratory "G. Savastano" of the University of Naples Federico II by means of a Haefely TEAS 570 detector, using the direct method arrangement, with a PD free coupling capacitor $C_s = 100$ pF and, as a test object, an HV bushing, with a capacitance $C_x \sim 80$ pF. The bandwidth of the detector was set at [40–400] kHz. Partial discharge signals detected by TEAS 570 were acquired using a Tektronix TDS5032B digitizer at a sampling frequency $f_s = 20$ MHz in a time window of 1 ms. The whole procedure consisted of three successive steps.

As a first step, calibration pulses were injected at the terminals of the test object using an external calibrator which gave the possibility to change the amplitude of the injected apparent charge and the time interval between two consecutive pulses. Examples of the recorded calibration signals are shown in Figure 10 in which, again, for better readability the time scales have been changed. Since the HV laboratory is a controlled EM environment, the signal to noise ratio is sufficiently high (SNR > +15 dB).

In the second step, the whole measuring setup was taken out from the laboratory and exposed to external noise and interferences. Again, the calibration signals were injected at the test object terminals, and the output from the detector was recorded.

In the third and last steps, PD pulses were extracted by wavelet transform using the *db14*. Typical experimental results are shown in Figure 11(a) and Figure 11(b) in which, respectively, one pulse and two consecutive pulses were reconstructed. The de-noising performances are quite satisfactory since after
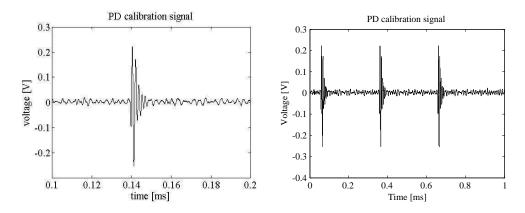
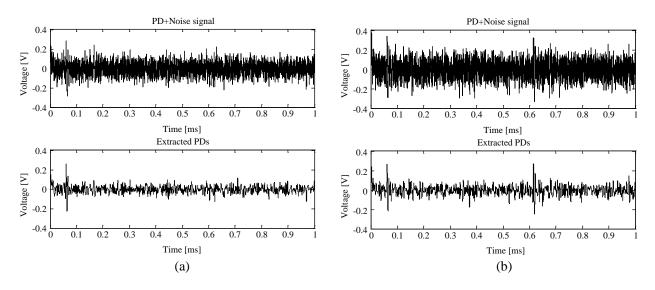**Figure 10.** Experimental PD calibration signal waveforms.

Figure 11. PD extraction in experimental tests. (a) One calibration pulse and (b) two calibration pulses.

the de-noising process the PD magnitudes (that is the peak values of recorded signals) are characterized by an average value $pce = 80\%$ while the correlation between the original and the extracted waveforms is described by an average value $pce = 42\%$.

Better performances can probably be obtained by selecting a deeper decomposition level with respect to the 5th level reached in the present paper. In such a case, since the energy of the signal is split in more than one node, a more suitable representation of PD waveforms could be given by the Wavelet Packet Transform (WPT) which allows a more detailed analysis with respect to Discrete Wavelet Transform (DWT), producing, for each generated node, an approximation and a detail subsequence. In this sense, work is in progress towards a comparison between WT and WPT. Further activity is directed towards the definition of the *Performance Fingerprint*, which could be improved by adding new performance parameters, such as the Mean Square Error (*mse*), or by giving different weights to those already defined. Last but not least, great effort will be dedicated to the exploitation of the wide potentialities of wavelets in PD measurements as for in the case of Partial Discharges in winding systems [25] which could be studied and identified with the help of a multiconductor transmission line model [26, 27] in conjunction with the Wavelet Transform.

5. CONCLUSIONS

An improved methodology was proposed for the selection of the best wavelet to be used for the extraction of partial discharges from noise and disturbances that employ a traditional wide-band partial discharge detector. It makes use of the *Performance Fingerprint*, a set mathematical operators that characterize the ability of a specific wavelet to reconstruct a partial discharge waveform. A distance criterion is then applied in order to select the most suitable wavelet. The performance of the applied technique was evaluated both in numerical and experimental tests. Encouraging results have been obtained even in extremely noisy environment. Work is in progress also to perform experimental tests on suitable specimen, and in particular, on artificially created defects in a noisy environment. Results will be compared with experimental data obtained in a screened laboratory in order to strictly verify the effectiveness of the de-noising method.

REFERENCES

1. Kreuger, F. H., *Partial Discharge Detection in High Voltage Equipment,* Butterworths, London, 1989.
2. Bartnikas, R., "Corona pulse counting and pulse-height analysis techniques," *Engineering Dielectrics, Volume I, Corona Measurement and Interpretation*, Chapter 9, R. Bartnikas, and E. J. Mc Mahon (eds.), STP 669, ASTM, Philadelphia, 1979.
3. Angrisani, L., P. Daponte, C. Dias, and A. Vale, "Advanced processing techniques of high-voltage impulse test signals," *IEEE Trans. on Instrumentation and Measurement*, Vol. 47, No. 2, 439–445, Apr. 1998.
4. Onal, E. and J. Dikun, "Short-time Fourier transform for different impulse measurements," *Balkan Journal of Electrical & Computer Engineering*, Vol. 1, No. 1, 44–47, 2013.
5. Shim, I., J. J. Soraghan, and W. H. Siew, "Digital signal processing applied to the detection of partial discharge: An overview," *IEEE Electrical Insulation Magazine*, Vol. 16, No. 3, 6–12, 2000.
6. Lupò, G., C. Petrarca, M. Vitelli, L. Angrisani, and M. Daponte, "Analysis of ultrawide-band detected partial discharges by means of a multiresolution digital signal-processing method," *Measurement, Journal of the International Meas. Confederation*, Vol. 27, No. 3, 207–221, 2000.
7. Cody, M. A., "The wavelet packet transform extending the wavelet transform," *Dr. Dobb's Journal*, M&T Publishing Inc., Apr. 1994.
8. Angrisani, L., M. D'Arco, M. Di Lorenzo del Casale, and C. Petrarca, "Extraction of PD data from UWB measurements on motor stator bars fed by an IGBT inverter," *2002 Conference on Electrical Insulation and Dielectric Phenomena (CEIDP)*, 844–847, Cancun, Mexico, 2002.
9. Petrarca, C., "The use of wavelet packet transform for digital-signal processing of PD data acquired from tests on inverter-fed specimen," *2004 International Conference on Solid Dielectrics (ICSD)*, Vol. 2, 892–895, Toulouse, France, 2004.
10. Petrarca, C. and G. Lupò, "Wavelet packet denoising of partial discharge data," *2006 Conference on Electrical Insulation and Dielectric Phenomena (CEIDP)*, 644–647, Kansas City, 2006.
11. Baki, A. K. M. and N. C. Karmakar, "Improved method of node and threshold selection in wavelet packet transform for UWB impulse radio signal denoising," *Progress In Electromagnetics Research C*, Vol. 38, 241–257, 2013.
12. Satish, L. and B. Nazneen, "Wavelet-based denoising of partial discharge signals buried in excessive noise and interference," *IEEE Trans. on Dielectrics and Electrical Insulation*, Vol. 10, No. 2, 354–367, 2003.
13. Zhou, X., C. Zhou, and B. G. Stewart, "Comparisons of discrete wavelet transform, wavelet packet transform and stationary wavelet transform in denoising PD measurement data," *2006 IEEE International Symposium on Electrical Insulation (ISEI)*, 237–240, Toronto, Canada, 2006.
14. Ma, X., C. Zhou, and I. J. Kemp, "Interpretation of wavelet analysis and its application in partial discharge detection," *IEEE Trans. on Dielectrics and Electrical Insulation*, Vol. 9, No. 3, 446–457, 2002.

15. Zhou, X., C. Zhou, and I. J. Kemp, "An improved methodology for application of wavelet transform for partial discharge measurement denoising," *IEEE Trans. on Dielectrics and Electrical Insulation*, Vol. 12, No. 3, 586–594, 2005.

16. Kyprianou, A., P. L. Lewin, V. Efthimiou, A. Stavrou, and G. E. Georghiou, "Wavelet packet denoising for online partial discharge detection in cables and its application to experimental field results," *Meas. Sci. Technol.*, Vol. 17, 2367–2379, IOP Publishing Ltd., 2006.

17. Chang, C. S., J. Jin, S. Kumar, Q. Su, T. Hoshino, M. Hanai, and N. Kobayashi, "Denoising of partial discharge signals in wavelet packet domain," *IEE Proc. — Sci. Meas. Technology*, Vol. 152, No. 3, 129–140, 2005.

18. Macedo, E. C. T., D. B. Araujo, E. G. da Costa, R. C. S. Freire, W. T. A. Lopes, I. S. M. Torres, J. M. R. de Souza Neto, S. A. Bhatti, and I. A. Glover, "Wavelet transform processing applied to partial discharge evaluation," *Journal of Physics: Conference Series*, Vol. 364, 1–16, IOP Publishing Ltd., 2012.

19. Sarkar, T. K., et al., "A tutorial on wavelets from an electrical engineering perspective, Part 1: Discrete wavelet techniques," *IEEE Antennas and Propagation Magazine*, Vol. 40, No. 5, 49–70, 1998.

20. Mallat, S., "A theory for multi-resolution signal decomposition: The wavelet representation," *IEEE Patt. Anal. Mach. Intell.*, Vol. 11, No. 7, 674–693, 1989.

21. Kreuger, F. H., *Industrial High Voltage, Volume II*, Delft University Press, 1992.

22. Morshuis, P. H. F., "Partial discharge mechanisms," Ph.D. Thesis, Delft University Press, 1993.

23. Gulski, E., "Computer-aided recognition of partial discharges using statistical tools," Ph.D. Thesis, Delft University Press, 1991.

24. Krivda, A., "Recognition of discharges: discrimination and classification," Ph.D. Thesis, Delft University Press, 1995.

25. Wood, J. W., H. G. Sedding, W. K. Hogg, I. J. Kemp, and H. Zhu, "Partial discharges in HV machines; initial considerations for a PD specification," *IEE Proceedings-A*, Vol. 140, No. 5, 409–416, 1993.

26. Petrarca, C., A. Maffucci, V. Tucci, and M. Vitelli, "Analysis of the voltage distribution in a motor stator winding subjected to steep-fronted surge voltages by means of a multiconductor lossy transmission line model," *IEEE Trans. on Energy Conversion*, Vol. 19, No. 1, 7–17, 2004.

27. De Vivo, B., P. Lamberti, V. Tucci, and C. Petrarca, "Simulation of the bearing voltage in an inverter-FED induction motor by a full three phase multi conductor transmission line model," *Progress In Electromagnetics Research B*, Vol. 46, 233–250, 2013.